Available online at www.sciencedirect.com
ScienceDirect
Geochimica et Cosmochimica Acta 73 (2009) 1523–1537
Geochimica et Cosmochimica Acta
www.elsevier.com/locate/gca

Possible impact-induced refractory-lithophile fractionations in EL chondrites

Alan E. Rubin [a,*], Heinz Huber [a], John T. Wasson [a,b,c]

[a] Institute of Geophysics and Planetary Physics, University of California, Los Angeles, CA 90095-1567, USA
[b] Department of Earth and Space Sciences, University of California, Los Angeles, CA 90095, USA
[c] Department of Chemistry and Biochemistry, University of California, Los Angeles, CA 90095, USA

Received 7 November 2007; accepted in revised form 2 December 2008; available online 13 December 2008

Abstract

Literature data show that refractory-lithophile elements in most chondrite groups are unfractionated relative to CI chondrites; the principal exception is the EL-chondrite group whose observed falls (all of which are type 6) are depleted in Ca and light REE. In contrast, literature data and our new INAA data on EL3 PCA 91020, EL3 MAC 88136 and EL4 Grein 002 show that some replicates of these samples have nearly flat REE patterns (unlike those of EL6 chondrites); other replicates exhibit fractionated REE patterns similar to those of EL6 chondrites. Petrographic examination shows that many EL6 (and some EL3 and EL4) chondrites are impact-melt breccias or contain impact-melted portions. We suggest that the same impact processes that formed these breccias and produced melt are responsible for the observed bulk compositional fractionations in refractory-lithophile elements, i.e., EL6 chondrites were produced from initially unequilibrated EL3 material. When large amounts of impact heat were deposited, plagioclase and/or oldhamite (CaS) (the major REE carriers in enstatite chondrites) may have been melted and then transported appreciable (>10 cm) distances. EL6 chondrites represent the residuum that is depleted in REE (particularly in LREE) and Ca. Unlike the case for EL chondrites, our new INAA data on ALH 84170, EET 87746 and SAH 97096 (all EH3) show some scatter but are consistent with the EH group having uniform refractory-lithophile abundances.

1. INTRODUCTION

Nearly all chondrite groups have uniform abundances of refractory-lithophile elements (e.g., Wasson and Kallemeyn, 1988), a property these rocks inherited from the solar nebula. Abundance ratios normalized to mean CI carbonaceous chondrites and to Mg range from ~1.4 in mean CV chondrites to 0.5 in mean EH chondrites; they are constant within analytical uncertainties for different individuals in each chondrite group irrespective of petrologic type. The sole reported exception is the EL enstatite–chondrite group; Kallemeyn and Wasson (1986) determined the bulk compositions of five EL6 chondrites by instrumental neutron-activation analyses (INAA) and found that these rocks are depleted in rare-earth elements (REE) and in Ca relative to other refractory-lithophile elements (e.g., Al and Sc). The REE themselves are fractionated, with abundances of light REE (LREE) such as La showing moderate depletions relative to heavy REE (HREE) such as Yb and Lu (e.g., Fig. 1 of Wasson and Kallemeyn, 1988).

EL chondrites of petrologic type <6 are all finds and were recognized only after the Kallemeyn and Wasson (1986) study was published: EL3 (MAC 88136; Lin et al., 1991); EL4 (QUE 94368; Rubin, 1997a); EL5 (Tanezrouft 031 and TIL 91714; Rubin et al., 1997). [Although Sears et al. (1984) and Zhang et al. (1994, 1996) suggested that RKP A80259 was an EL5 chondrite on the basis of its low siderophile-element content and the cathodoluminescence color of enstatite, Rubin et al. (1997) classified it as EH5 on the basis of its high La/Sm ratio, small mean

* Corresponding author. Fax: +1 310 206 3051.
E-mail address: aerubin@ucla.edu (A.E. Rubin).

0016-7037/$ - see front matter © 2008 Elsevier Ltd. All rights reserved.
doi:10.1016/j.gca.2008.12.002

chondrule size and sulfide mineralogy (it contains keilite [(Fe,Mg)S] rather than ferroan alabandite [(Mn,Fe)S]). Kallemeyn and Wasson (1986) attributed the low siderophile-element content of RKP A80259 to terrestrial weathering and leaching.]

Petrologic studies have shown that many EL6 chondrites have suffered complex parent-body processes including shock heating, incomplete melting, brecciation and annealing (Rubin, 1983a,b, 1984, 1997a,b; Rubin et al., 1997). The aim of the present study was to explore the possibility that the fractionated compositions of EL6 chondrites are a secondary characteristic resulting from parent-body processing. We studied a suite of EL3 and EL4 chondrites petrographically to evaluate evidence of impact melting. We chose three relatively unaltered samples (EL3 PCA 91020, EL3 MAC 88136 and EL4 Grein 002) for analysis by INAA and augmented our results with literature data.

EH3–5 chondrites appear to be isochemical irrespective of petrologic type (Kallemeyn and Wasson, 1986). To confirm this result and facilitate comparisons between EH3 and EL3 chondrites, we analyzed three EH3 chondrites by INAA (ALH 84170, EET 87746 and SAH 97096).

2. ANALYTICAL PROCEDURES

We examined thin sections of 11 EL3 and EL4 chondrites petrographically in transmitted and reflected light: EET 90992,6 – EL3; Grein 002 – EL4 (UCLA 1863); LAP 03930,4 – EL3; MAC 88136,29 – EL3; MAC 02635,6 – EL3; MAC 02747,7 – EL4; MAC 02837,8 – EL3; PCA 91020,15 – EL3; QUE 93351,5 – EL3; QUE 94321,4 – EL3; and QUE 94368,4 – EL4. All of the thin sections except the UCLA section of Grein 002 are of Antarctic meteorites (obtained from NASA – Johnson Space Center).

We analyzed two replicates each of EH3 ALH 84170, EH3 EET 87746, EH3 Sahara 97096 (hereafter SAH 97096), EL3 PCA 91020 and EL4 Grein 002, and a single sample of EL3 MAC 88136 by INAA. Data for 29 elements were obtained. Meteorites belonging to other chondrite groups (CM, CO, H) were included in the runs and their REE distributions were found to be within established ranges. Samples were generally analyzed as 3-mm thick rectangular prisms. The sawn surfaces were cleaned with SiC paper; rusty patches on other surfaces were flaked off with stainless steel dental picks. Sample masses were in the range of 150–424 mg (Table 1).

Samples were irradiated for 3 h at the TRIGA Mark I reactor of the University of California, Irvine with a lazy-susan flux of 1.8×10^{12} neutrons cm^{-2} s^{-1} for the determination of isotopes with half-lives of several hours and more. For counting, the samples were mounted on cardboard slides. Counting distances and shapes of the samples were approximately the same as those of the powdered material used as standards. Standards included the Allende meteorite (Jarosewich et al., 1987), the USGS international reference materials granite G-2 and BHVO-1 (Govindaraju, 1994), as well as elemental solutions pipetted onto MgO (for Os, Ir and Au). Analyses were carried out following a protocol similar to that of Kallemeyn et al. (1989).

A subsequent short irradiation in the pneumatic facility at the UC-Irvine reactor was performed to determine the abundances of elements with short-lived isotopes (e.g., Al, Mg and Ti). Samples were irradiated for 60 s and counted for 250 s after a cooling period of 300 s. Standards used in this procedure included the USGS international reference materials BHVO-1, BIR-1 (Govindaraju, 1994) and the Allende meteorite (Jarosewich et al., 1987). We monitored calibration errors by comparing the results of the Allende standard from each individual INAA run. The relative sample standard deviations determined from the Allende sample are less than 5% for most elements; Ca and K have standard deviations of ±6% and ±8%, respectively. Errors for Os and Ru are relatively high, 10–15%.

Throughout the paper we use the terms "flat", "uniform" and "unfractionated" interchangeably when referring to a group of elements with similar abundances.

3. RESULTS

3.1. Petrographic evidence for shock effects in EL3 and EL4 chondrites

Impact-melted enstatite chondrites are characterized by euhedral grains of enstatite encased within nodules consisting of metal and/or sulfide, euhedral graphite blades, and partly resorbed chondrules with surfaces that appear to have served as nucleation sites for euhedral enstatite grains crystallizing from the melt (e.g., Rubin, 1997b; Rubin and Scott, 1997; Rubin et al., 1997; Patzer et al., 2004; Keil, 2007). Most of the EL3 and EL4 chondrites examined in the present study contain impact-melted regions; some of these chondrites have been largely melted.

In EET 90992 and PCA 91020 (both EL3), ~20% of the round metal nodules contain euhedral enstatite grains. Both meteorites also contain regions wherein massive sulfide surrounds angular silicate debris. In PCA 91020, the surfaces of some of the chondrules appear to have served as nucleation sites for euhedral enstatite grains.

MAC 02837 (EL3) contains a large patch of sulfide surrounding numerous euhedral enstatite grains. Material in the rest of the thin section appears unmelted.

In MAC 88136 (EL3), many of the metal nodules in one 2.4 × 6.8-mm size region of the thin section contain euhedral enstatite grains; some of these nodules also contain euhedral graphite blades. The metal nodules in the other regions of the thin section are free of euhedral enstatite and appear unmelted.

Sulfide-rich melts containing abundant angular and rounded silicate grains surround many of the chondrules in the EL3 chondrites MAC 02635, QUE 93351 and QUE 94321.

The EL4 chondrites show more extensive melting than the majority of EL3 chondrites. Most of the metal nodules in MAC 02747 contain euhedral enstatite grains; large numbers of euhedral enstatite grains occur in the metal throughout QUE 94368 and Grein 002. Chondrule surfaces in these rocks served as nucleation sites for some euhedral enstatite grains crystallizing from the melt. Impact-melted portions of QUE 94368 and Grein 002 also contain

Table 1
Individual results of replicate INAA analyses and whole-rock averages of EL and EH chondrites.

	PT	mass, mg	Na, mg/g	Mg, mg/g	Al, mg/g	K, μg/g	Ca, mg/g	Sc, μg/g	Ti, μg/g	V, μg/g	Cr, mg/g	Mn, mg/g	Fe, mg/g	Co, μg/g	Ni, mg/g	Zn, μg/g	Ga, μg/g	As, μg/g	Se, μg/g	Ru, μg/g	Sb, ng/g	La, ng/g	Sm, ng/g	Eu, ng/g	Yb, ng/g	Lu, ng/g	Os, ng/g	Ir, ng/g	Au, ng/g
EL chondrites																													
PCA 91020	3	310.4	6.50	131	11.1	789	9.15	7.62	967	50.7	3.21	1.72	277	886	16.2	101	11.3	2.48	18.9	0.94	142	164	134	55.8	173	26.3	765	610	287
PCA 91020	3	157.8	5.68	134	11.4	596	10.6	7.02	927	50.2	2.93	1.82	219	669	13.3	93	8.2	1.93	13.2	0.87	90	311	183	68.3	201	30.0	437	450	197
PCA 91020-av	3		6.09	132	11.2	693	9.86	7.32	947	50.44	3.07	1.77	248.18	778	14.7	97.1	9.75	2.21	16.1	0.91	116.17	238	158	62.1	187	28.1	601	530	242
MAC 88136[a]	3		5.61	130	9.69	768	9.94	6.83	800	52.8	2.80	1.72	251	777	14.9	138	12.9	2.57	19.3	0.91	155	284	163	68.8	194	29.7	778	599	257
Grein 002	4	405.2	6.78	143	11.1	684	11.7	6.99	175	53.9	2.79	1.77	240	726	13.9	226	11.1	2.15	21.0	0.88	161	317	176	72.7	206	31.9	726	586	240
Grein 002	4	423.9	6.92	145	10.7	748	10.1	7.33	818	42.7	2.78	1.69	260	819	17.5	223	12.8	4.24	18.1	1.09	133	208	172	75.3	219	33.8	688	659	267
Grein 002-av	4		6.85	143	10.9	716	10.9	7.16	497	48.2	2.78	1.73	250	773	15.7	225	12.0	3.20	19.5	0.99	147.09	262	174	74.0	212	32.8	707	623	254
EH chondrites																													
Sahara 97096	3	326.0	6.89	127	9.63	804	9.30	6.47	305	54.5	3.55	2.37	313	885	17.4	309	15.3	3.55	25.4	0.94	191	243	153	63.3	187	27.3	699	615	322
Sahara 97096	3	353.5	6.35	98.1	8.38	813	7.65	5.56	569	49.4	2.90	1.97	285	841	16.1	308	13.6	2.84	22.3	0.91	155	245	153	54.6	141	22.3	609	554	296
Sahara 97096-av	3		6.62	113	9.00	808	8.47	6.02	437	51.9	3.23	2.17	299	863	16.8	309	14.5	3.20	23.9	0.92	173	244	153	59.0	164	24.8	654	585	309
EET 87746	3	149.7	6.28	105	9.07	779	8.30	5.48	582	50.5	3.04	2.06	292	848	15.8	357	12.0	2.93	26.0	0.86	216	263	139	52.8	154	25.0	640	560	309
EET 87746	3	296.0	5.60	125	8.53	850	8.54	5.60	719	49.2	3.13	1.86	290	858	17.5	357	16.8	3.33	21.9	0.75	194	230	127	67.1	172	27.7	701	578	352
EET 87746-av	3		5.94	115	8.80	815	8.42	5.54	650	49.8	3.08	1.96	291	853	16.6	357	14.4	3.13	24.0	0.80	205	246	133	59.9	163	26.3	670	569	331
ALH 84170	3	275.5	5.33	116	8.90	703	7.76	5.61	654	42.4	2.75	1.86	265	803	13.7	260	14.6	2.49	22.6	0.94	186	268	161	66.5	176	26.9	591	534	281
ALH 84170	3	168.0	4.94	125	9.42	721	8.13	6.04	737	47.2	3.01	1.54	281	818	16.6	294	15.1	3.14	19.2	0.99	170	278	155	65.1	187	31.2	878	608	346
ALH 84170-av	3		5.13	121	9.16	712	7.95	5.83	695	44.8	2.88	1.70	273	811	15.1	277	14.8	2.81	20.9	0.96	178	273	158	65.8	182	29.1	735	571	313

PT, petrologic type; av, average.
[a] Only a single analysis.

euhedral grains of sinoite and graphite (Rubin, 1997a, 2006; Patzer et al., 2004).

In contrast to the other EL3 and EL4 chondrites, the small (8.8 g) EL3 chondrite LAP 03930 is highly chondritic and contains no euhedral enstatite grains. The available material appears to have escaped impact melting.

3.2. Bulk compositions

3.2.1. EH chondrites

Mean EH chondrites (Fig. 1) have relatively unfractionated abundances of refractory-lithophile elements including REE (Kallemeyn and Wasson, 1986). Interelement fractionations among the REE are unresolvable. To facilitate the discussion of element fractionations in our new analyses of EH and EL chondrites, we normalized our data to the Kallemeyn–Wasson (1986) EH3–5 mean in Figs. 2 and 3. The Kallemeyn–Wasson EL6 mean abundance ratios are shown as a reference line. Our new INAA data on the EH3 chondrites ALH 84170, EET 87746 and SAH 97096 (Table 1 and Fig. 2a) yield Mg-normalized abundance-ratio patterns similar to those for EH chondrites (Kallemeyn and Wasson, 1986), although the abundance ratios in Cr, Mn, Na and K in ALH 84170 are intermediate between EH and EL. The average La/Sm abundance ratios of the three meteorites are 1.09, 1.18 and 1.00, respectively. The mean EH- and Mg-normalized abundance ratios and standard deviations of the five REE in the three EH3 chondrites are La: 1.02 ± 0.06, Sm: 1.04 ± 0.10, Eu: 1.08 ± 0.07, Yb: 1.05 ± 0.07 and Lu: 1.08 ± 0.08, respectively. The moderately high values of the refractory-lithophile elements suggest that our Mg abundances are, on average, a few percent lower than those of Kallemeyn and Wasson (1986).

With the exception of one replicate each of SAH 97096 and EET 87746, the abundances of Mn and the alkalies (Na and K) are lower in the new EH3 data set than in mean EH and the scatter is large (Fig. 2a). The abundances in ALH 84170 are close to the EL6 pattern.

Nickel-normalized abundances of refractory-siderophile elements (Fig. 3a) are similar to mean EH for EET 87746 and SAH 97096. Abundances of Ru and Os in ALH 84170 show an EL-like pattern, but our errors are large for these elements. The volatile and chalcophile abundances scatter; Zn is somewhat higher in all the EH3 data, but within the range observed by Kallemeyn and Wasson (1986). In particular, the previous values for ALH A77295, Indarch, Kota–Kota and St. Sauveur are in the same range. Sears et al. (1983) observed similar Zn values in some clasts in Abee.

Because of the scatter observed among some of our replicates, we augmented our data with analyses of an EH3 (ALH 84170) and an EL3 (MAC 88136) chondrite from the data set published by Kong et al. (1997); these are plotted with unfilled symbols having the same shapes used for our data for these same meteorites. To minimize the clutter on the diagrams, we limited our use of such data to chondrites for which we had only one replicate or where we observed larger degrees of scatter. On the Ni-normalized plots (Fig. 3) we found that the Kong et al. data plotted distinctly lower than ours, implying systematic differences in Ni. To facilitate the comparison of their data with ours, we increased the plotted Kong et al. values by 10% to compensate partially for this difference; this adjustment shows up on the diagrams as Ni values plotting above unity.

3.2.2. EL chondrites

3.2.2.1. EL6 chondrites. Kallemeyn and Wasson (1986) analyzed five EL6 chondrites including four falls (Hvittis, Jajh deh Kot Lalu, Khairpur, Pillistfer) and one Antarctic find (ALH A81260) that was characterized as "relatively unweathered" (weathering grade A/Be; Grady, 2000). Mean EL6 chondrites in this data set show fractionated refractory-lithophile abundances (Fig. 2): Ca and REE abundances are low, with LREE lower than HREE. Note that Al and Sc are not depleted.

The mean abundance and standard deviation of the set of five EL6 REE (normalized to CI chondrites and to Mg) is 0.82 ± 0.07. The La/Yb abundance ratio in the EL6 chondrite falls (0.79 ± 0.11; Table 2) illustrate the depletion in LREE; the corresponding value in mean EH3–5 chondrite falls is 1.04 ± 0.05. The mean EL6 La/Sm abundance ratio is 0.89 ± 0.07, in contrast to the EH-chondrite ratio of 1.10 ± 0.03 (Table 2).

The Ca depletion in EL6 chondrites is reflected in the relatively low Ca/Al and Ca/Sc abundance ratios (0.90 ± 0.08 and 0.86 ± 0.08, respectively); the corresponding (unfractionated) ratios in EH3–5 chondrites are 0.99 ± 0.04 and 0.97 ± 0.08 (Table 2). The Ca/Mg abundance ratios in mean EL6 and mean EH3–5 chondrites are 0.75 ± 0.07 and 0.84 ± 0.04, respectively (Table 2).

The siderophile and chalcophile data are best compared as Ni-normalized abundance ratios (Fig. 1c). Here the most interesting feature is that, relative to the common elements Ni, Fe and Co, refractory siderophiles (Os, Ir, Ru) are 20–25% higher in EL, whereas the volatile siderophiles (Au, As, Ga) are lower by factors of 5–15%.

Magnesium-normalized abundance ratios of the chalcophile–volatile elements Cr, Mn, Na, K, Se and Zn in mean EL6 chondrites (Figs. 2 and 3) relative to those in EH chondrites range from ~0.7 for Cr and Na to 0.4 for Se and 0.06 for Zn. Although Zn abundances vary widely in both EL and EH chondrites (Table 1; Kallemeyn and Wasson, 1986), the mean difference is a factor of 16, far larger than can be accounted for by sample heterogeneity or analytical uncertainty.

3.2.2.2. EL3 and EL4 chondrites. Prior to the present study, literature data were available for three EL3 chondrites – ALH 85119 (two samples), MAC 88136 (five samples including the paired meteorites MAC 88180 and MAC 88184) and PCA 91020 (one sample) (Zhang et al., 1995; Kong et al., 1997). Most of these analyses show less-fractionated refractory-lithophile patterns than the EL6 chondrites.

In order to confirm and extend these results, we analyzed replicate samples of EL3 PCA 91020 and EL4 Grein 002, and a single sample of EL3 MAC 88136 (Table 1). The EH- and Mg-normalized lithophile data are plotted in Fig. 2b. The mean refractory-lithophile patterns are much less fractionated than that of mean EL6. Although the

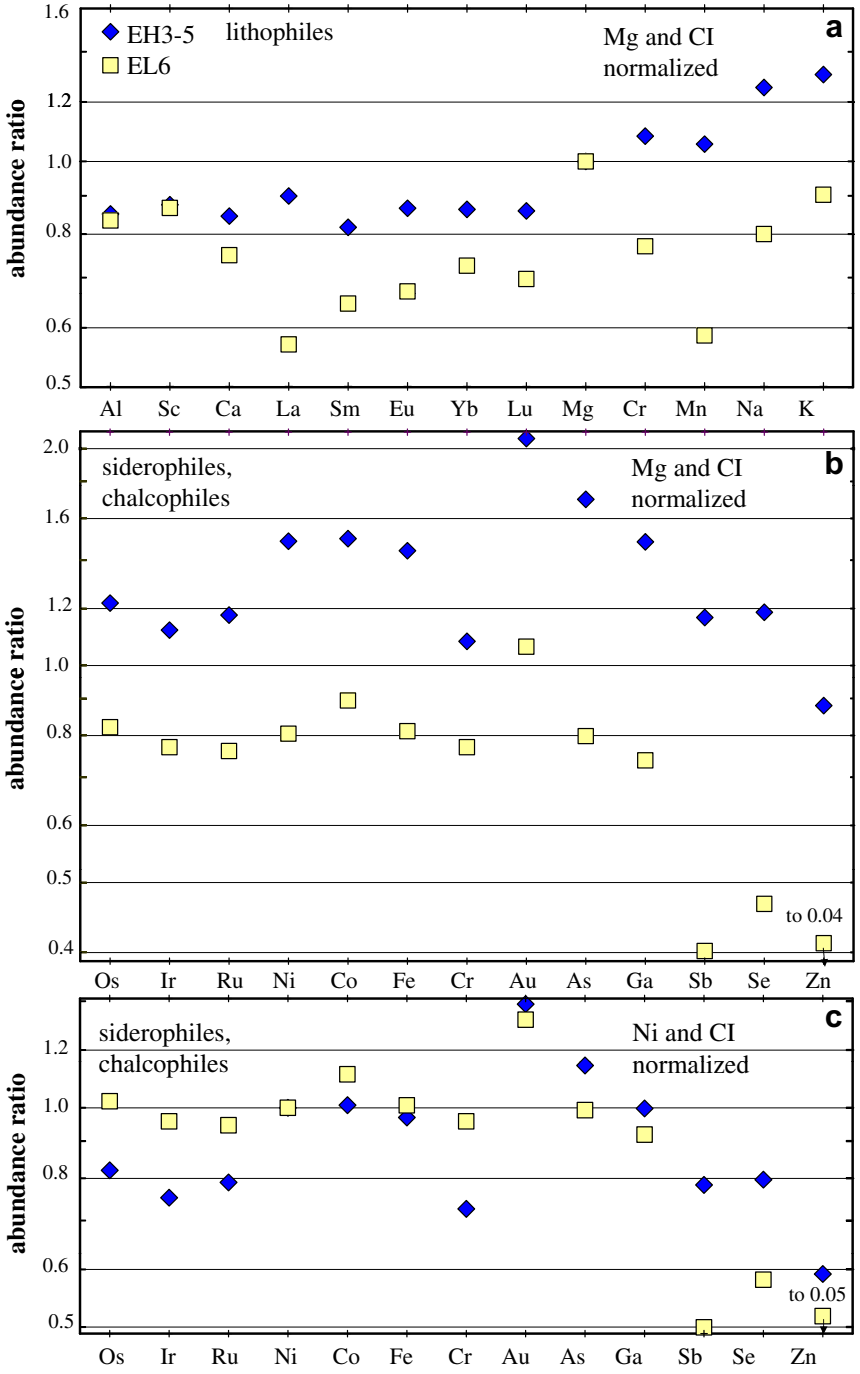

Fig. 1. Bulk compositions of mean EH3–5 chondrites and mean EL6 chondrites determined by INAA. Data from Kallemeyn and Wasson (1986). (a) "Lithophile" elements normalized to CI chondrites and to Mg. Elements are listed from left to right in order of increasing volatility. EH chondrites (filled diamonds) have essentially unfractionated refractory "lithophile" element abundances. EL6 chondrites (open squares) are depleted in LREE, particularly La; they are also depleted in Eu relative to Yb and Lu. The EL6 chondrites show a low abundance of Mn (a moderately volatile element). (b) Siderophiles and chalcophiles normalized to CI chondrites and to Mg. These two geochemical varieties of elements are listed separately from left to right in order of increasing volatility. EH3–5 chondrites contain much higher abundances of these elements than EL6 chondrites. This difference is an important parameter distinguishing the two groups. The label 0.04 at bottom right refers to the square symbol attached to a downward-pointing arrow and represents the Mg- and CI-normalized Zn abundance ratio of EL6 chondrites. (c) Siderophiles and chalcophiles normalized to CI chondrites and to Ni. These two varieties of elements are listed separately from left to right in order of increasing volatility. EL6 chondrites show enhanced abundances of refractory siderophiles, low to very low abundances of most moderately volatile siderophiles, and very low abundances of Se and Zn compared to EH chondrites. The label 0.05 at bottom right refers to the square symbol attached to a downward-pointing arrow and represents the Ni- and CI-normalized Zn abundance ratio of EL6 chondrites.

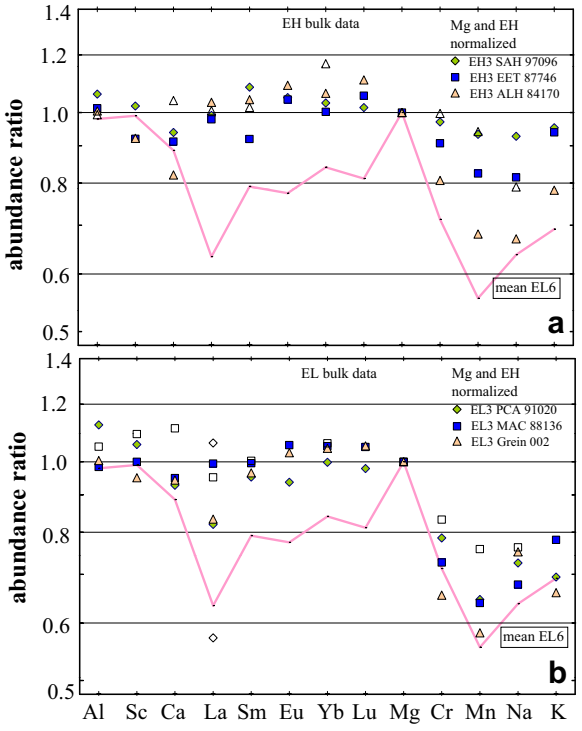

Fig. 2. Bulk compositions of lithophile elements in EH3, EL3, EL4 and mean EL6 chondrites determined by INAA. (a) Average bulk compositions of three EH3 chondrites normalized to mean EH chondrites and to Mg. Mean EL6 chondrites (data from Kallemeyn and Wasson, 1986) are plotted as a line labeled "mean EL6". Although the EH3 chondrites appear to be more depleted in Mn than mean EH chondrites, their refractory-lithophile-element abundances are not distinguishable from those of more-equilibrated EH chondrites. EH chondrites appear to be nearly isochemical irrespective of petrologic type. (b) Average bulk compositions of three EL3 chondrites (and mean EL6 chondrites) normalized to mean EH chondrites and to Mg. The open squares represent data for MAC 88136 from Kong et al. (1997). Open diamonds show individual La analyses of PCA 91020; one sample has a high abundance and one a low abundance of many lithophile elements.

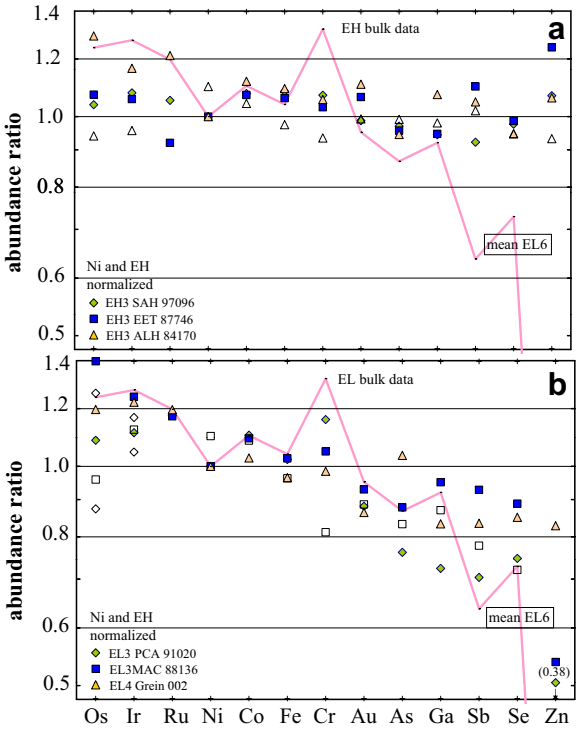

Fig. 3. Bulk compositions of siderophile and chalcophile elements in enstatite chondrites determined by INAA and normalized to EH3–5 chondrites (Kallemeyn and Wasson, 1986) and to Ni. These two geochemical varieties of elements are listed separately from left to right in order of increasing volatility. Mean EL6 chondrites are plotted as a thick line in each diagram. The value for the EL6 Zn abundance ratio (0.08) falls below the diagram and is not plotted. EL6 chondrites are depleted in volatile siderophiles and chalcophiles relative to refractory siderophiles. We include Cr because it fractionates in a manner similar to that of the common siderophile elements. The data of Kong et al. (1997) are shown as open symbols; we arbitrarily increased their Ni values by 10% to bring the abundances of other siderophile elements closer to those of our data to facilitate comparisons. (a) EH3 chondrites have essentially unfractionated abundances of siderophile and chalcophile elements relative to mean EH chondrites, indicating that the EH group is essentially isochemical for these elements irrespective of petrologic type. (b) EL3 and EL4 chondrites have siderophile-element abundance patterns similar to that of mean EL6 chondrites, but have appreciably higher abundances of chalcophile elements. Although the Cr/Mg abundance ratio among EL3 and EL4 chondrites is less than unity (Fig. 2b), there is no evident depletion in the Cr/Ni abundance ratio.

mean La abundances in Grein 002 and PCA 91020 are 16–18% lower than mean EH values, a wide scatter is observed between replicates; in Fig. 2b, the PCA 91020 replicates are plotted as light-gray diamonds, those for Grein 002 are similar, but less extreme. Noteworthy is that the PCA 91020 sample with the high La abundance has 25–30% lower abundances of most volatiles and chalcophiles. These large sampling variations make it impossible to determine the true abundance patterns, but it seems that these are more similar to flat (unfractionated) patterns than to the Kallemeyn–Wasson EL6 pattern.

Although the Ca abundance ratios in the EL3 and EL4 samples are about 5% low compared to the mean EH fall value, the EH3 abundances were similarly depleted. This important discrepancy requires further investigation. Our interpretation is that the mean EL-chondrite Ca abundance is the same within error as the mean EH-chondrite Ca abundance.

Manganese is the "lithophile" showing the lowest abundance ratio in the EL3 and EL4 samples. Although Mn is plotted with the lithophiles, a sizable fraction is present in sulfides in EH and EL chondrites (e.g., Keil, 1968). (We estimate that 77% of the Mn in EH3 chondrites occurs in sulfides.) Mean values of Mn in EL3 and EL4 replicates are higher than the EL6 mean, but by small factors (5–20%) and are within the range of Mn abundances in EL3 and EL4 chondrites observed previously.

The EH- and Mg-normalized Cr abundance ratios in EL3 and EL4 chondrites (Fig. 2b) are the same as reported by Kallemeyn and Wasson (1986) for EL6 falls and are

Table 2
CI- and Mg-normalized elemental abundance ratios in EL6 and EH3–5 chondrites.

	La/Yb	Eu/Yb	Sm/Yb	La/Sm	Ca/Al	Ca/Sc	Ca/Mg	Mn/Mg	Se/Mg	Zn/Mg	Na/Mg	K/Mg
EL6	0.79	0.92	0.89	0.89	0.90	0.86	0.75	0.59	0.47	0.04	0.80	0.90
EH3–5	1.05	1.01	0.95	1.10	1.00	0.97	0.85	1.05	1.19	0.65	1.26	1.31

Enstatite–chondrite data from Kallemeyn and Wasson (1986); CI-chondrite data from Wasson and Kallemeyn (1988).

much (1.4×) lower than those in EH falls. On average, the EL3 and EL4 Na values are 12% higher than in mean EL6 falls and the EL3 and EL4 K values are the same as EL6 within experimental scatter.

In Fig. 3b we show Ni-normalized abundances of EL3 and EL4 siderophiles and chalcophiles. Abundance ratios of the three refractory siderophiles are high, similar to mean EL6 values for Grein 002 and MAC 88136, and intermediate between EL and EH for PCA 91020. The single determination of Os in MAC 88136 is high, but there are relatively large sampling and analytical errors. To illustrate these, we plot as open diamonds our replicate Os and Ir values for PCA 91020; the Os replicates differ by a facor of ~1.3, the Ir values by a factor of ~1.1.

Abundance ratios of the common siderophile elements Co and Fe in EL3 and EL4 chondrites are consistent with either EH or EL, but Au values are similar to, although slightly lower than, EL values. Abundance ratios of As and Ga scatter about or near the EL ratios.

Abundance ratios of Sb and Se scatter above mean EL and below mean EH. Kallemeyn and Wasson (1986) observed relatively little scatter in EL6 Zn; their mean concentration and sample standard deviation are 18 ± 5 μg/g. Our abundance ratios in EL3 and EL4 finds scatter. The MAC 88136 and PCA 91020 values are low, but higher than those in EL falls. The mean Zn abundance ratio in Grein 002 is much higher still, i.e., $0.84 \times$ EH.

4. DISCUSSION

4.1. Classification and elemental fractionations among type-3 enstatite chondrites

The EH3 and {EL3 plus EL4} chondrites that we studied are clearly members of two different groups based on their EH- and Mg-normalized siderophile-element abundances. The mean EH- and Mg-normalized abundance ratios of Ni, Co and Fe in our three EH3 chondrites are in the range 0.87–0.95, whereas the range for our three EL3 and EL4 samples is 0.68–0.73.

Plots of EH-normalized element/Mg ratios of Ni, Fe and Au vs. that of Co (Fig. 4) demonstrate that the EH and EL groups are fully resolved (although one replicate of EL PCA 91020 plots near the lowest EH replicates). The other PCA 91020 replicate is one of the two lowest points on the diagrams (the other is a replicate of EL4 Grein 002). Our sample sizes were typically only 200–300 mg; thus, it is possible that individual samples may not contain representative amounts of metal. Our interpretation of these data is that there is strong evidence that EH and EL planetesimals have resolvably different abundances of these four elements (Ni, Fe, Au, Co), and that these differences were established in the solar nebula, reflecting formation at different times and/or locations.

In the following section, we will examine the possibility that several of the elemental fractionations recorded in EL6 chondrites were produced by shock-induced mobilization of phases (mainly sulfides) and migration to distal regions outside the analyzed whole-rock samples. Our working hypothesis is that the type-3 chondrites were affected to a lesser extent by these processes.

We assume that all EL materials were initially unshocked (and compositionally unfractionated) type-3 chondrites; those particular samples that were most strongly affected by shock processes were transformed into recrystallized and compositionally fractionated EL6 chondrites. EL4 chondrites were, on average, shocked more than EL3 chondrites. The available EL3 chondrites experienced different degrees of shock melting. Those EL3 materials that largely escaped impact melting remained compositionally unfractionated, type-3 rocks.

It is important to examine whether some elemental fractionations might have been present at the time planetesimals formed in the nebula. In Section 3, we showed our lithophile-element abundances normalized to Mg and our siderophile- and chalcophile-element abundances normalized to Ni.

With these considerations in mind, we conclude that (with the exception of a 10–15% depletion in La) the refractory-lithophile abundance ratios (Al through Lu) plotted in Fig. 2a and b show no resolvable differences between {EL3 plus EL4} chondrites and EH3 chondrites. The mean CI- and Mg-normalized abundance ratios for the nine refractory-lithophile elements in Table 1 (Al, Ca, Sc, Ti, La, Sm, Eu, Yb, Lu) are 0.92 ± 0.12 for the three EH3 chondrites and 0.91 ± 0.15 for the three EL3 + EL4 chondrites (Table 1).

The Ti data appear to be anomalously high and we exclude this element from further consideration. If Ti is excluded from the refractory lithophile mean, the CI- and Mg-normalized ratios of the remaining eight elements for the EH3 and EL3–4 chondrites are 0.89 ± 0.06 and 0.86 ± 0.05, respectively. It thus appears that, with the exception of La, the EL3 refractory-lithophile pattern is basically flat and that, within error, the mean refractory-lithophile abundance ratio of EL3 chondrites is the same as that in EH3 chondrites. [An analogous situation pertains to the ordinary chondrites (OC). Although differing in their CI- and Mg-normalized abundance ratios of siderophiles, the H, L and LL chondrites have very similar CI- and Mg-normalized abundance ratios of refractory lithophiles (Fig. 7 of Kallemeyn et al., 1989). The similarities in refrac-

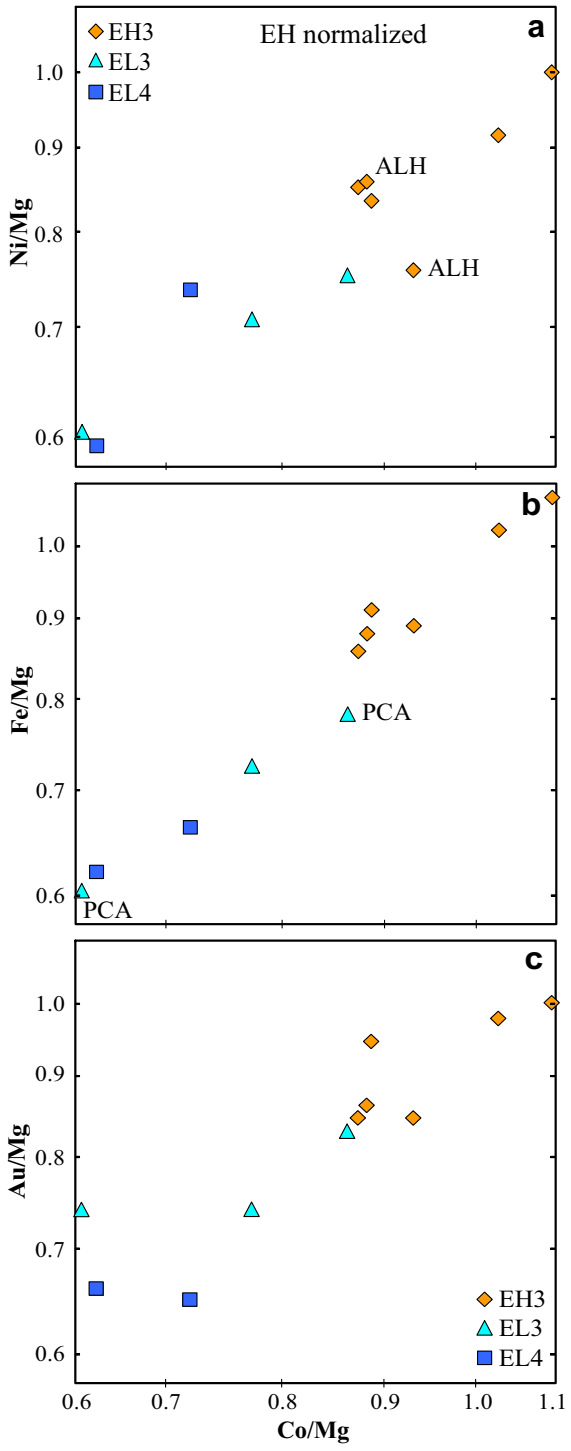

Fig. 4. EH- and Mg-normalized plots of three siderophile elements (Ni, Fe, Au) vs. Co for EH3, EL3 and EL4 chondrites. (The EH normalization is from the EH3–5 mean of Kallemeyn and Wasson, 1986.) Positive correlations indicate that the siderophile elements are concentrated in the same components and that the abundance of these components varies from sample to sample. The two replicates of EH3 ALH 84170 (labeled ALH) show moderate variability in Ni/Mg vs. Co/Mg; the two replicates of EL3 PCA 91020 (labeled PCA) show large differences in Fe/Mg vs. Co/Mg. These data support the assignment of these unequilibrated chondrites to their respective EH (high siderophile) or EL (low siderophile) groups.

tory lithophiles among members of the enstatite–chondrite clan and among members of the ordinary-chondrite clan were inherited from the solar nebula.]

It is routinely surmised that members of each chondrite group were derived from a single parent asteroid (e.g., McSween, 1987). Hence, EL3, EL4 and EL5 chondrites are assumed to be members of the same chondrite group as EL6 chondrites and are thought to be derived from the same body. The assignment of these chondrites to the same group is based on their mineralogical and textural similarities. The EL3, EL4 and chondrule-bearing EL6 chondrites all have relatively large-diameter chondrules (~550 μm) compared to ~220-μm diameter chondrules in EH chondrites (Rubin, 2000). All of the EL chondrites have kamacite with relatively low Si contents (0.12–1.7 wt% vs. 2.2–3.5 wt% in EH; Keil, 1968; Rambaldi et al., 1983; Lin et al., 1991) and contain ferroan alabandite [(Mn,Fe)S] instead of the niningerite [(Mg,Fe)S] or keilite [(Fe,Mg)S] that occurs in EH chondrites (e.g., Keil, 1968, 2007; Lin et al., 1991). Consistent with the supposition that all of the EL chondrites were derived from the same parent asteroid are the similarities in the cosmic-ray-exposure age distributions of EL3 and EL6 chondrites (Fig. 5 of Patzer and Schultz, 2001).

The high-petrologic-type members of each chondrite group are inferred to have formed from material compositionally and texturally akin to that of low-petrologic type members (e.g., Van Schmus and Wood, 1967). Thus, because the refractory-lithophile abundance patterns in EL3 chondrites are flat (with the exceptions of small depletions of Ca and La), the fractionation pattern observed in EL6 chondrites is unlikely to be nebular. Another explanation is required.

A possible hypothesis is that shock processes on the EL parent body were responsible for these compositional fractionations. To help evaluate this model, we first discuss the petrologic evidence for shock in these rocks.

4.2. Shock effects

4.2.1. EL6 chondrites

Most EL6 chondrites have textures that appear to have been produced by shock melting and/or brecciation. A few prominent examples are discussed here. Hvittis is a fragmental breccia containing ~5 vol % impact-melt-rock clasts, the largest of which is 2.5 cm in diameter (Fig. 1 of Rubin, 1983a). Blithfield is a chondrule-free (Easton, 1983), highly recrystallized, impact-melt breccia consisting of multi-centimeter-size metal-poor, sulfide-rich clasts embedded in a metal-rich matrix containing metal veins and centimeter-size metal nodules (Fig. 1 of Rubin, 1984). Atlanta is a breccia containing a centimeter-size sulfide-rich clast; kamacite veins up to 2.5 cm in length transect the matrix (Rubin, 1983b; Fig. 2 of Rubin et al., 1997). Eagle is a breccia containing fine-grained, centimeter-size black inclusions (probably formed by silicate darkening due to the shock melting and concomitant dispersion of small blebs of metal and sulfide) (Olsen et al., 1988; Rubin et al., 1997). University of Hawaii thin section UH163 of Jajh deh Kot Lalu contains a 2 × 16-mm size plagioclase-bear-

ing, chondrule-free vein that is rich in oldhamite (CaS) (Fig. 3 of Rubin et al., 1997). The vein may be an impact-melt product.

Euhedral enstatite grains and euhedral graphite laths are characteristic of EH-chondrite impact-melt breccias; these phases crystallized from the shock melt (e.g., Rubin, 1997a,b; Rubin and Scott, 1997; McCoy et al., 1999). Many EL6 chondrites also contain euhedral grains of enstatite and graphite (e.g., NWA 2213, Forrest 033, GRO 95626, QUE 97462, Neuschwanstein), suggesting that these rocks may be annealed impact-melt breccias (Rubin et al., 1997; Bischoff and Zipfel, 2003; Rubin, 2006).

Rubin (1997a) identified euhedral grains of sinoite (Si_2N_2O) in impact-melted portions of the QUE 94368 EL4 chondrite (Fig. 5) and proposed that sinoite formed by crystallization from EL-chondrite impact melts (see below). Similarly, Bischoff et al. (2005) reported sinoite in an EL impact-melt rock (Ilafegh 009).

Small rare grains of sinoite occur as inclusions in keilite (Karwowski et al., 2007) in the Zaklodzie meteorite, an enstatite-rich rock that contains kamacite grains with an average concentration of 1.5 wt% Si (Pryzlibski et al., 2005). The abundant polysynthetically twinned clinoenstatite grains in Zaklodzie indicate quenching and suggest that this meteorite is an enstatite–chondrite impact-melt rock (Burbine et al., 2000). The relatively low Si content of the kamacite suggests that it may have been derived from an EL chondrite.

Euhedral sinoite grains are present in numerous EL6 chondrites (Forrest 033, Hvittis, Jajh deh Kot Lalu, Neuschwanstein, Pillistfer, Ufana, Yilmia, ALH A81021, ALH 83018, EET 90102, GRO 95626, LEW 88714, LON 94100). As inferred above from the presence of euhedral enstatite and graphite in many of these rocks, the occurrence of sinoite is also supportive of the suggestion that these meteorites are impact-melt breccias (Rubin, 1997a, 2006; Bischoff et al., 2005).

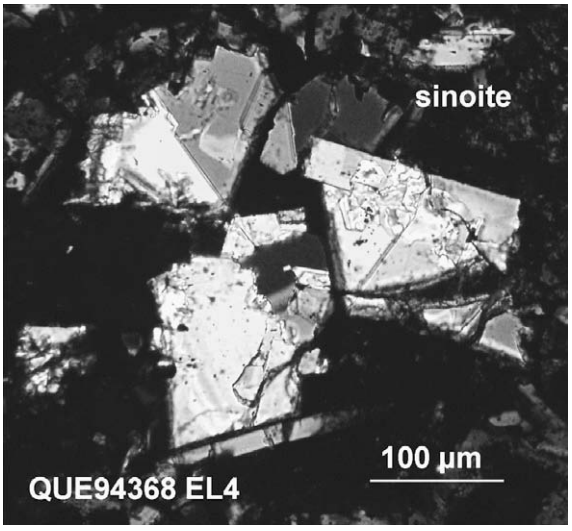

Fig. 5. Highly birefringent, euhedral and intergrown sinoite grains in an impact-melted portion of EL4 QUE 94368. Transmitted light, crossed nicols.

Despite the fact that many EL6 chondrites appear to have experienced impact-melting and/or brecciation, the majority of these rocks are designated shock-stage S2 (very weakly shocked) (Rubin et al., 1997; Rubin, 2006) as indicated by undulose extinction in orthopyroxene and the absence of clinoenstatite lamellae parallel to (100) (a characteristic of shock-stage S3). Rubin et al. (1997) inferred that many EL6 chondrites had been appreciably shocked and melted, and then buried and annealed beneath insulating, low-porosity ejecta. During annealing, the orthopyroxene crystal lattices would have healed, giving the rocks the appearance of shock-stage S1 (i.e., unshocked) materials. Subsequent low-energy impacts caused the orthopyroxene grains to develop undulose extinction, increasing their apparent shock-stage to S2.

4.2.2. EL5 chondrite

Bischoff et al. (2005) reported sinoite in one EL5 chondrite (TIL 91714), a shock-stage S2 rock (Rubin et al., 1997). This suggests that this rock also could be an annealed impact-melt breccia. These workers did not find sinoite in the only other EL5 chondrite that they examined (i.e., Tanezrouft 031, also shock-stage S2).

4.2.3. EL4 chondrites

Approximately 10–15 vol% of EL4 QUE 94368 consists of portions that appear to have been impact melted (Rubin, 1997a). These regions contain euhedral enstatite grains and euhedral graphite laths, similar to those throughout the Abee EH impact-melt breccia (Rubin and Keil, 1983; Rubin et al., 1997). The impact-melted regions of QUE 94368 also contain euhedral grains of sinoite (Fig. 5). The occurrence of sinoite in other EL chondrites with impact-melted areas and in the Ilafegh 009 EL impact-melt rock prompted Bischoff et al. (2005) to support the impact-melt model of Rubin (1997a) for the formation of sinoite.

Portions of Grein 002 (EL4) have also experienced impact melting (Fig. 6). These regions contain euhedral grains of enstatite, graphite and sinoite (Patzer et al., 2004; Rubin, 2006). Many of the euhedral enstatite grains in Grein 002 are surrounded by metal clasts or nodules (Patzer et al.,

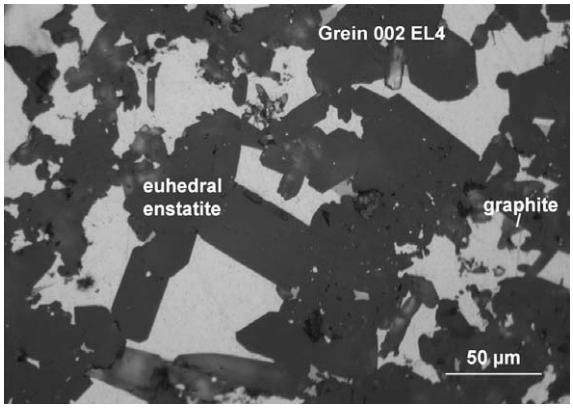

Fig. 6. Impact-melted portion of EL4 Grein 002 showing euhedral enstatite grains and small euhedral graphite laths surrounded by kamacite (white). Reflected light.

2004; Rubin, 2006) as in Abee (Dawson et al., 1960; Rubin and Keil, 1983; Rubin et al., 1997) and in the Ilafegh 009 and Y-86004 enstatite–chondrite impact-melt rocks (McCoy et al., 1995; Lin and Kimura, 1998).

MAC 02747 (EL4) also contains euhedral grains of enstatite and graphite (Rubin, 2006). The section we examined is transected by several 2–3-mm long metal shock veins.

4.2.4. EL3 chondrites

PCA 91020 (EL3) is shock-stage S5 (Rubin et al., 1997); it is one of the most highly shocked enstatite chondrites. Maskelynite is present. PCA 91020 also contains rapidly solidified metal-troilite assemblages (cf. Scott, 1982) with 4–10-μm size metal spheroids surrounded by troilite (Fig. 7). The meteorite has a foliation (as do some other EL3 chondrites; e.g., MAC 02635 and EET 90992); ellipsoidal chondrules, elongated chondrule fragments and elongated opaque assemblages exhibit a preferred orientation. Foliations in OC and CR chondrites are attributed to impact deformation (Sneyd et al., 1988; Lee et al., 1992) and it seems probable that impacts are also responsible for the foliations in EL3 chondrites.

MAC 88136 is a breccia (Lin et al., 1991) of shock-stage S3 (Rubin et al., 1997). Metal nodules containing euhedral enstatite grains occur in ~20 vol % of the rock, indicating that these portions have probably experienced impact melting. However, extensive *late-stage* impact melting of this rock is precluded by the presence of excess ^{53}Cr in Mn-bearing sphalerite (El Goresy et al., 1992) because if such melting had occurred, the sphalerite also would have melted and the isotopes would have homogenized.

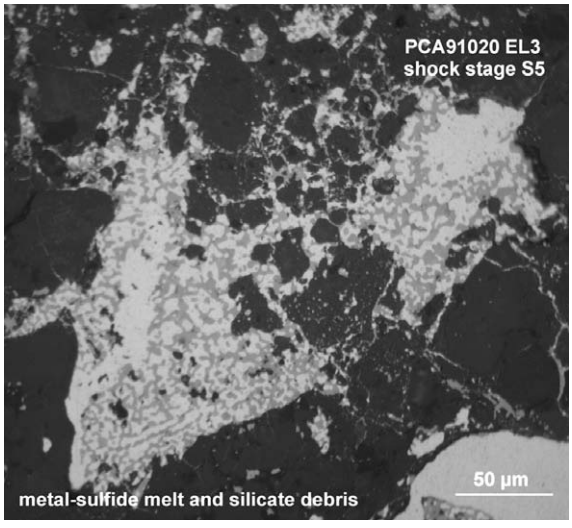

Fig. 7. Melted and rapidly solidified assemblage of metal (white) and sulfide (light gray) in the shock-stage S5 EL3 chondrite PCA 91020. Adjacent silicate grains (dark gray) contain numerous small blebs of metal and sulfide that probably were melted and injected into fractures in the silicate grains during the impact event(s). Reflected light.

4.3. Causes of compositional fractionations in EL chondrites

4.3.1. Possible models

We examine two possible models to explain the compositional differences between EL and EH chondrites. In both cases, we infer that physical fractionations of components were involved: (1) Compositional differences between EL and EH chondrites resulted from mechanical fractionations of solid components that occurred in the solar nebula. (2) The compositional differences between these groups resulted from parent-body processes involving fractionations of impact melts from residual solids.

4.3.2. Dismissal of the nebular model for REE fractionation

As discussed above, with the exception of La, our EL3 and EL4 samples show only minor fractionations among refractory-lithophile elements. If EL6 chondrites were formed from EL3 material (as is widely assumed), then the fractionated patterns in EL6 chondrites were not completely produced in the nebula.

4.3.3. Evaluation of non-nebular models for REE fractionation

Because many of the elements that are fractionated in EL chondrites are, in part, associated with sulfide, our working model is that the missing fractions of Ca and REE (and possibly a fraction of some additional elements e.g., Na, K, Mn, Zn, Se) were in sulfides (or plagioclase) that were not present in the analyzed samples of EL6 chondrites (e.g., Kallemeyn and Wasson, 1986).

We envision different possible reasons for the absence of these elements from the analyzed samples: (1) the sulfides are water soluble, and large fractions were lost as a result of terrestrial weathering or sample-preparation procedures involving water; (2) a sizable fraction of the sulfides formed large (>1 cm) segregations that experienced extensive attrition during the destruction of the parent asteroid or during atmospheric passage; and (3) parent-body impact processes melted and mobilized the sulfides (and some plagioclase) which migrated appreciable distances (centimeters to meters) and were largely excluded from the analyzed portions of the meteorites.

4.3.3.1. Effects of terrestrial weathering and sample preparation. It is improbable that the EL6 fractionation pattern (Figs. 1 and 2) was produced by terrestrial weathering or sample-preparation procedures. Most of the analyzed EL6 chondrites are observed falls and exhibit little weathering. Because oldhamite (CaS) is the major carrier of REE in enstatite chondrites (Larimer and Ganapathy, 1987; Lundberg and Crozaz, 1988; Floss and Crozaz, 1993) and because this mineral is soluble in water (e.g., Merrill, 1915), it is necessary to explore the possibility that the depletions in LREE and Ca in EL6 chondrites are due nonetheless to terrestrial weathering of the samples or to sample-preparation techniques involving water as a lubricant.

Some samples of the Antarctic EL3 chondrites have essentially unfractionated REE abundances and significantly higher Ca than EL6 chondrites. Some have moderately high terrestrial ages and tend to be relatively small

(recovered masses of MAC 88136 and PCA 91020 were 74.4 and 1749 g, respectively). Grein 002 (EL4) is from Niger and had an initial mass of 609 g. In contrast, the EL6 falls with fractionated REE abundances tend to be appreciably larger (Hvittis – 14 kg; Jajh deh Kot Lalu – 973 g; Khairpur – 13.6 kg; Pillistfer – 23.25 kg). Terrestrial weathering should have affected small EL3 and EL4 finds to a much greater extent than large EL6 falls; the small EL3 and EL4 chondrites have higher surface/volume ratios, they presumably have a higher porosity, and they have much longer terrestrial ages. Furthermore, the relatively small (124 g) ALH 81260 EL6 find analyzed by Kallemeyn and Wasson (1986) shows the same REE fractionations as the EL6 falls; the CI- and Mg-normalized ratios in ALH 81260 and the EL6 falls are La/Sm = 0.83 and 0.88 ± 0.07; La/Yb = 0.85 and 0.79 ± 0.11; Eu/Yb = 0.94 and 0.91 ± 0.07, respectively. It seems clear that loss of oldhamite due to weathering is not mainly responsible for the Ca depletion or the REE fractionations of the EL6 chondrites.

Antarctic meteorite samples are routinely cut using water as a lubricant, a procedure allowing the possibility of oldhamite dissolution and concomitant loss of REE and Ca. However, because some of these samples have less fractionated REE abundances and higher Ca abundances than the EL6 falls (many of which were also exposed to water in the laboratory), the ubiquitous depletions in Ca and REE in EL6 chondrites are unlikely to be artifacts of sample preparation.

4.3.3.2. Attrition of sulfide-rich segregations. There is a paucity of S-rich magmatic iron meteorites relative to the numbers expected if differentiated parent bodies of chondritic bulk composition were sampled representatively (e.g., Kracher and Wasson, 1982). It seems likely that sulfide-rich iron meteorites formed, but because such samples would be more friable than S-poor irons, they may have been selectively destroyed during impact-excavation from their parent asteroid or, conceivably, by ablation during atmospheric passage.

Oldhamite-rich enstatite–chondrite impact-melt rocks and breccias may have been subject to similar modes of attrition. Samples containing appreciable oldhamite may have formed during impact melting but may have been winnowed out prior to arriving at the surface of the Earth.

4.3.3.3. Impact-induced depletions in LREE, Ca and Eu. We favor a model wherein impacts are mainly responsible for causing the EL6 depletions in LREE, Ca and Eu. For proper evaluation of the loss mechanism for LREE and Eu, it is necessary to determine where the REE are sited in primitive EL and EH chondrites. Of particular importance is knowledge of the fraction of La in common EL phases. Lanthanum is the largest and most incompatible lanthanide; it has the smallest mineral–melt partition coefficient for common minerals (which tend to have small cation coordination sites) (e.g., Henderson, 1996). Among the trivalent LREE, La tends to fractionate to a greater degree during crystallization of minerals from a melt.

REE abundances are high in oldhamite in EH3 and EL3 chondrites (10–100 × CI; Floss and Crozaz, 1993; Crozaz and Lundberg, 1995). About 70% of the individual oldhamite grains characterized by Floss and Crozaz (1993) as "unweathered" have relatively flat REE patterns; ~30% of these grains are enriched in LREE, particularly La (Fig. 9 of Floss and Crozaz, 1993; Figs. 2–5 of Crozaz and Lundberg, 1995).

Other phases in enstatite chondrites that contain measureable amounts of La include plagioclase, enstatite and diopside. Plagioclase is enriched in LREE and commonly has a positive Eu anomaly (e.g., Fig. 2 of Floss and Crozaz, 1993; Fig. 7 of Hsu, 1998). Some enstatite grains in EH3 chondrites have relatively flat REE patterns; others are depleted in LREE (Figs. 1 and 2 of Hsu and Crozaz, 1998). Diopside in aubrites and EL6 chondrites tends to be depleted in LREE (Fig. 3 of Floss and Crozaz, 1993; Fig. 3 of Floss et al., 2003).

The mean La concentration in EL3 oldhamite (23.2 ± 6.2 μg/g, $n = 10$; Table 2 of Crozaz and Lundberg, 1995) is ~230 times higher than that in EL6 plagioclase (0.102 μg/g) or diopside (0.10 μg/g) (Tables 1–3 of Floss and Crozaz, 1993). This discrepancy is only partially compensated for by the higher modal abundance of plagioclase than oldhamite; for example, the Hvittis EL6 chondrite fall contains only 25 times more plagioclase than oldhamite (5.2 vs. 0.21 wt%; Rubin, 1983a). The modal abundance of diopside in EL3 chondrites is low (Lin et al., 1991), almost certainly <1 wt%.

The picture is similar in EH chondrites. The mean La concentration in EH3 oldhamite (17.8 ± 5.0 μg/g, $n = 22$; Table 2 of Crozaz and Lundberg, 1995) is 60 times higher than the mean La concentration in EH3 enstatite (0.298 μg/g; Hsu and Crozaz, 1998). This discrepancy is only partially compensated for by the higher modal abundance of enstatite; e.g., EH3 ALH A77156 contains 69 vol % clinoenstatite and 1.6 vol % oldhamite (McKinley et al., 1984) and thus ~50 times more enstatite than oldhamite (after the data are converted into weight-percent using mineral densities from Keil, 1968 and Nickel and Nichols, 1991). The amount of plagioclase in EH3 Y 791790 is ~5.4 wt% (data from Kimura and Lin, 1999 converted into weight-percent).

In order to estimate the proportions of La in different phases in enstatite chondrites, we assume the following modal abundances and La concentrations of enstatite–chondrite minerals (43.5 wt% enstatite with 0.298 μg/g La; 6.6 wt% plagioclase with 0.102 μg/g La; 0.95 wt% oldhamite with 23.2 μg/g La; 0.70 wt% diopside with 0.10 μg/g La). We further assume that no other phases contain significant amounts of La; this assumption is consistent with the failure to detect La in ferroan alabandite in EL3 MAC 88136 and in niningerite in ALH A77156 (Table 5 of Crozaz and Lundberg, 1995). We calculate that 62% of the La in enstatite chondrites is in oldhamite, 36% is in enstatite, 1.9% is in plagioclase and 0.2% is in diopside.

Because most EH3 and EL3 oldhamite grains have REE patterns that are either relatively flat or LREE enriched (Crozaz and Lundberg, 1995), loss of oldhamite from EL chondrites would deplete the whole rocks in REE, particu-

larly LREE. It would also deplete the whole rocks in Ca. The modal abundances and mineral compositions of chondrule-rich clasts in the Adhi Kot EH breccia (Rubin, 1983c) and the mineralogy of EH3 ALH A77156 (McKinley et al., 1984) and EH3 Qingzhen (Grossman et al., 1985) indicate that most of the Ca (we estimate ~64%) in enstatite chondrites is in oldhamite. [Smaller proportions of Ca occur in plagioclase (or feldspathic chondrule mesostases) (~7%) and pyroxene (clinoenstatite, orthoenstatite and diopside) (~26%); very small proportions (0.3–1.4%) of Ca occur in forsterite, troilite and niningerite.]

The low La/Yb and Ca/Mg abundance ratios in mean EL6 chondrites and in the fractionated samples of EL3 and EL4 chondrites are thus qualitatively consistent with loss of oldhamite from these rocks. In view of (1) the petrographic evidence in many of these rocks for impact melting (Rubin, 1983a,b, 1984, 1997a, 2006; Rubin et al., 1997; Patzer et al., 2004) and (2) the concentration of oldhamite in objects that have been inferred to be impact-melt products (i.e., the chondrule-free vain in Jajh deh Kot Lalu and the dark inclusions in Abee; Rubin and Keil, 1983; Rubin et al., 1997), we conclude that the low La/Yb and Ca/Mg abundance ratios in many EL chondrites were caused by loss of oldhamite due to impact melting and mobilization.

The EH- and Mg-normalized La/Mg ratio in EL6 chondrites is 0.63 (Fig. 2b); if oldhamite contains 62% of the La in EL6 chondrites (and if EH chondrites and EL6 chondrites initially had the same oldhamite concentration), then ~60% of the oldhamite would had to have been lost from EL6 chondrites to achieve this La/Mg ratio. Loss of this much oldhamite would also have caused the EH- and Mg-normalized Ca/Mg ratio in EL6 chondrites to drop from 1.00 to 0.62 × EH. Because plagioclase in EL6 chondrites typically contains only 3–4 wt% CaO (Rubin 1983a,b, 1984), loss of some plagioclase along with oldhamite would further diminish the Ca/Mg abundance ratio only slightly. The result of these calculations (Ca/Mg = 0.62 × EH in EL6 chondrites) is in relatively poor agreement with the observed EL6 Ca/Mg ratio of 0.89 × EH (Fig. 2b). It therefore seems likely that less oldhamite was lost from EL6 chondrites and that the lost oldhamite had a higher mean La content than that of EL3 MAC 88136 (23.2 μg/g).

The chondrule-free oldhamite-rich vein in Jajh deh Kot Lalu (Fig. 3 of Rubin et al., 1997) contains much more oldhamite than the whole rock (6.7 vs. 0.8 wt%). It also contains large (500 × 700 μm) polycrystalline clumps of plagioclase. This implies that both oldhamite and plagioclase were melted and mobilized during shock melting.

Objects that may be related to the oldhamite-rich vein are the oldhamite-rich, plagioclase-bearing "dark inclusions" in the Abee EH-chondrite impact-melt breccia (Rubin and Keil, 1983); these objects appear to be impact-melt products. The Abee dark inclusions are significantly enriched in Ca and REE relative to Mg and mean EH chondrites and have negative Eu anomalies (Fig. 5 of Sears et al., 1983). One of the two dark inclusions (SI 2096) analyzed by Sears et al. (1983) is depleted in La relative to Sm and Lu; the other (9,13,1) is not.

Although oldhamite is a highly refractory phase with a melting temperature of ~2800 K (Chase et al., 1985), it can melt at lower temperatures in conjunction with other phases (e.g., 1800–1900 K in the system CaO–MgO–SiO_2–CaS; Rudneva and Panov, 1962). Oldhamite also appears to be soluble in melts of enstatite–chondrite composition (Fogel et al., 1996). McCoy et al. (1999) conducted partial melting experiments on EH4 Indarch and found that complete melting of sulfide and metal occurred at or below ~1300 K.

Most investigated oldhamite grains in EH chondrites have relatively flat REE patterns; those in EL6 chondrites (while otherwise flat) have significant negative Eu anomalies (Fig. 7 of Floss and Crozaz, 1993; Fig. 1 of Floss et al., 2003), consistent with their crystallization in equilibrium with plagioclase. (The oldhamite-dominated igneous clasts in the Norton County aubrite also have flat REE patterns with negative Eu anomalies; Wheelock et al., 1994.)

Among the 50 "unweathered" oldhamite grains in EH3 and EL3 chondrites analyzed by Floss and Crozaz (1993), 68% have relatively flat REE patterns with no significant Eu anomalies, 30% have significant positive Eu anomalies and 2% have small negative Eu anomalies. Plagioclase grains in enstatite chondrites are expected to have positive Eu anomalies (Crozaz and Lundberg, 1995) as they do in aubrites (e.g., Fig. 2 of Floss and Crozaz, 1993). The loss of some oldhamite and plagioclase during impact melting of EL chondrites would thus lead to whole-rock depletions in Eu as well as in Ca and LREE. This is consistent with the observed small depletions of Eu in EL6 chondrites (which have a mean EH- and Mg-normalized Eu/Yb abundance ratio of 0.92) as well as in the fractionated sample of EL3 PCA 91020 (wherein Eu/Yb = 0.91) (Fig. 2b).

It is clear that impact melting of EL chondrites can produce S-rich melts. Blithfield (EL6) contains multi-centimeter-size clasts with sulfide/metal ratios (wt%) of 3.8–4.9 (Table 1 of Rubin, 1984), an order of magnitude greater than that in typical EL6 whole rocks (0.38 ± 0.22) (Table 2 of Keil, 1968). Such fractionations seem possible in light of the partial melting experiments on EH4 Indarch by McCoy et al. (1999) which produced three immiscible metallic melts, two immiscible sulfide melts, and a silicate melt.

Localized impact processes cannot deplete the bulk asteroid in refractory "lithophile" elements; the missing elements may have ended up in plagioclase- and/or oldhamite-rich melts. The oldhamite-rich vein in Jajh deh Kot Lalu may represent an oldhamite-rich melt that migrated only a short distance (perhaps 1–10 cm) from the site where it formed. We speculate that other melts migrated somewhat larger distances and separated from those EL6 whole rocks represented in our collections. Regions containing these melts may have been excluded from the EL-chondrite materials in our collections.

4.3.4. Depletions in Na, K, Mn, Zn and Se

Relative to EH3–5 chondrite falls, EL6 falls have moderately low CI-normalized abundances of Na, K, Mn and Se and a very low abundance of Zn (Table 2): Mn/Mg = 1.05 ± 0.07 vs. 0.59 ± 0.16; Na/Mg = 1.25 ± 0.12 vs. 0.80 ± 0.02; K/Mg = 1.31 ± 0.18 vs. 0.90 ± 0.08; Se/Mg = 1.17 ± 0.09 vs. 0.47 ± 0.09; Zn/Mg = 0.65 ± 0.20 vs. 0.04 ± 0.01; in EH and EL chondrites, respectively (Kallemeyn and Wasson, 1986). Selenium and Zn are chalco-

phile in enstatite chondrites and Mn, Na and K are partly chalcophile. Sodium and K are also concentrated in plagioclase.

Loss of oldhamite, plagioclase, and possibly other sulfide phases from EL chondrites by impact melting and mobilization could conceivably account for the depletions of these elements in EL chondrites. Volatilization during impact events could also be partly responsible for the loss of some of these elements. By analogy, some interplanetary dust particles (IDPs) appear to have lost Zn, Se and other volatile elements via volatilization during atmospheric passage (e.g., Flynn and Sutton, 1992; Flynn et al., 1992).

Nevertheless, the case for the loss of Na, K, Mn, Zn and Se from EL6 chondrites by impact melting on the parent body is not compelling and fractionation by nebular processes must also be considered.

5. SUMMARY: IMPACT-INDUCED FRACTIONATIONS IN EL CHONDRITES

Most EL6 chondrites have textures that appear to have been affected by shock melting. For example, Blithfield is an impact-melt breccia consisting of metal-poor, sulfide-rich clasts surrounded by a metal-rich matrix, Hvittis is a breccia containing large impact-melt-rock clasts, and Jajh deh Kot Lalu contains a plagioclase-bearing, chondrule-free vein that is rich in oldhamite. Many EL6 chondrites contain euhedral grains of enstatite, graphite and sinoite (Si_2N_2O) that are characteristic of EL impact-melt breccias. Regions of many EL3 and EL4 chondrites also appear to have been shock melted. These regions typically contain metal nodules and euhedral enstatite grains; some also contain euhedral graphite blades and sinoite.

EL6 chondrites and some portions of EL3 and EL4 chondrites are depleted in Ca and LREE (particularly La) and Eu relative to EH chondrites. The CI- and Mg-normalized La/Yb and Sm/Yb abundance ratios in EL6 chondrites (0.79 and 0.89, respectively) are appreciably lower than the corresponding values in EH chondrites (1.05 and 0.95). The mean CI- and Mg-normalized EL6 La/Sm abundance ratio is 0.89; that in EH chondrites is 1.10. EL6 Ca/Al and Ca/Sc CI- and Mg-normalized abundance ratios (0.90 and 0.86) are lower than the EH values (1.00 and 0.97). These compositional fractionations were produced by the impact processes that formed the EL breccias. Metallic Fe–Ni, silicates and sulfides were partly melted in these rocks. When EL3 materials were sufficiently heated by impacts, a plagioclase- and oldhamite-bearing melt was transported away from the shocked rocks and were thus not included in analyzed samples. Batches of shock-heated EL3 materials that were buried beneath hot, low-porosity ejecta and appreciably annealed became EL6 chondrites. EL3 materials that survived and avoided extensive impact processing were not texturally annealed and remained largely unfractionated.

ACKNOWLEDGMENTS

We thank the curators at the NASA Johnson Space Center for the INAA specimens and for the loan of thin sections. We are also grateful to C. Floss for providing useful information on REE abundances in enstatite-rich meteorites. Reviews by C. Floss and two anonymous referees were helpful in revising the manuscript. We appreciate the numerous helpful comments offered by Associate Editor G.F. Herzog. This work was supported in part by NASA Cosmochemistry Grants NNG06GF95G (A.E. Rubin) and NNG06GG35G (J.T. Wasson).

REFERENCES

Bischoff A. and Zipfel J. (2003) Mineralogy of the Neuschwanstein (EL6) chondrite – first results. *Lunar Planet. Sci.* **34**, 1212 (abstr.).

Bischoff A., Grund T., Jording T., Heying B., Hoffman R.-D., Rodewald U. C. and Pöttgen R. (2005) Occurrence, structure, and formation of sinoite in enstatite chondrites (abstract). *Meteorit. Planet. Sci.* **40**, A20.

Burbine T. H., McCoy T. J. and Dickinson T. L. (2000) Origin of plagioclase-"enriched", igneous, enstatite meteorites (abstract). *Meteorit. Planet. Sci.* **35**, A36.

Chase M. W., Davies C. A., Downey J. R., Frurip D. J., McDonald R. A. and Syverud A. N. (1985) JANAF thermochemical tables, third edition. *J. Phys. Chem. Ref. Data* **14**(Suppl. 1), 1–1856.

Crozaz G. and Lundberg L. L. (1995) The origin of oldhamite in unequilibrated enstatite chondrites. *Geochim. Cosmochim. Acta* **59**, 3817–3831.

Dawson K. R., Maxwell J. A. and Parsons D. E. (1960) A description of the meteorite which fell near Abee, Alberta, Canada. *Geochim. Cosmochim. Acta* **21**, 127–144.

Easton A. J. (1983) Grain-size distribution and morphology of metal in E-chondrites. *Meteoritics* **18**, 19–27.

El Goresy A., Wadhwa M., Nagel H.-J., Zinner E. K., Janicke J. and Crozaz G. (1992) ^{53}Cr–^{53}Mn systematics of Mn-bearing sulfides in four enstatite chondrites (abstract). *Lunar Planet. Sci.* **23**, 331–332.

Floss C. and Crozaz G. (1993) Heterogeneous REE patterns in oldhamite from aubrites: their nature and origin. *Geochim. Cosmochim. Acta* **57**, 4039–4057.

Floss C., Fogel R. A., Lin Y. and Kimura M. (2003) Diopside-bearing EL6 EET 90102: insights from rare earth element distributions. *Geochim. Cosmochim. Acta* **67**, 543–555.

Flynn G. J. and Sutton S. R. (1992) Trace elements in chondritic stratospheric particles: zinc depletion as a possible indicator of atmospheric entry heating. In *Proc. Lunar Planet. Sci. Conf.* 22nd, pp. 171–184.

Flynn G. J., Sutton S. R., Thomas K. L., Keller L. P. and Klöck W. (1992) Zinc depletions and atmospheric entry heating in stratospheric cosmic dust particles. *Lunar Planet. Sci.* **23**, 375–376.

Fogel R. A., Weisberg M. K. and Prinz M. (1996) The solubility of CaS in aubrite silicate melts (abstract). *Lunar Planet. Sci.* **27**, 371–372.

Govindaraju K. (1994) Compilation of working values and descriptions for 383 geostandards. *Geostand. Newslett.* **118**, 1–158.

Grady M. M. (2000) *Catalogue of Meteorites*. Cambridge University Press, 689 pp.

Grossman J. N., Rubin A. E., Rambaldi E. R., Rajan R. S. and Wasson J. T. (1985) Chondrules in the Qingzhen type-3 enstatite chondrite: possible precursor components and comparison to ordinary chondrite chondrules. *Geochim. Cosmochim. Acta* **49**, 1781–1795.

Henderson P. (1996) The rare earth elements: introduction and review. In *Rare Earth Minerals: Chemistry, Origin and Ore Deposits* (eds. A. P. Jones, F. Wall and C. T. Williams).

Mineralogical Society Series 7, Chapman & Hall, London, pp. 1–19.

Hsu W. (1998) Geochemical and petrographic studies of oldhamite, diopside, and roedderite in enstatite meteorites. *Meteorit. Planet. Sci.* **33**, 291–301.

Hsu W. and Crozaz G. (1998) Mineral chemistry and the origin of enstatite in unequilibrated enstatite chondrites. *Geochim. Cosmochim. Acta* **62**, 1993–2004.

Jarosewich E., Clarke R. S. and Barrows J. N. (1987) The Allende meteorite reference sample. *Smithson. Contrib. Earth Sci.* **27**, 1–49.

Kallemeyn G. W. and Wasson J. T. (1986) Compositions of enstatite (EH3, EH4, 5 and EL6) chondrites: implications regarding their formation. *Geochim. Cosmochim. Acta* **50**, 2153–2164.

Kallemeyn G. W., Rubin A. E., Wang D. and Wasson J. T. (1989) Ordinary chondrites: bulk compositions, classification, lithophile-element fractionations, and composition-petrographic type relationships. *Geochim. Cosmochim. Acta* **53**, 2747–2767.

Karwowski L., Kryza R. and Przylibski T. (2007) New chemical and physical data on keilite from the Zaklodzie enstatite achondrite. *Am. Mineral.* **92**, 204–209.

Keil K. (1968) Mineralogical and chemical relationships among enstatite chondrites. *J. Geophys. Res.* **73**, 6945–6976.

Keil K. (2007) Occurrence and origin of keilite, $(Fe_{>0.5}, Mg_{<0.5})S$, in enstatite chondrite impact-melt rocks and impact-melt breccias. *Chem. Erde* **67**, 37–54.

Kimura M. and Lin Y. (1999) Petrological and mineralogical study of enstatite chondrites with reference to their thermal histories. *Antarct. Meteorit. Res.* **12**, 1–18.

Kong P., Mori T. and Ebihara M. (1997) Compositional continuity of enstatite chondrites and implications for heterogeneous accretion of the enstatite chondrite parent body. *Geochim. Cosmochim. Acta* **61**, 4895–4914.

Kracher A. and Wasson J. T. (1982) The role of S in the evolution of the parental cores of the iron meteorites. *Geochim. Cosmochim. Acta* **46**, 2419–2426.

Larimer J. W. and Ganapathy R. (1987) The trace element chemistry of CaS in enstatite chondrites and some implications regarding its origin. *Earth Planet. Sci. Lett.* **84**, 123–134.

Lee M. S., Rubin A. E. and Wasson J. T. (1992) Origin of metallic Fe–Ni in Renazzo and related chondrites. *Geochim. Cosmochim. Acta* **56**, 2521–2533.

Lin Y. and Kimura M. (1998) Petrographic and mineralogical study of new EH melt rocks and a new enstatite chondrite grouplet. *Meteorit. Planet. Sci.* **33**, 501–511.

Lin Y. T., Nagel H.-J., Lundberg L. L. and El Goresy A. (1991) MAC88136 – the first EL3 chondrite (abstract). *Lunar Planet. Sci.* **22**, 811–812.

Lundberg L. L. and Crozaz G. (1988) Enstatite chondrites: a preliminary ion microprobe study (abstract). *Meteoritics* **23**, 285–286.

McCoy T. J., Keil K., Bogard D. D., Garrison D. H., Casanova I., Lindstrom M. M., Brearley A. J., Kehm K., Nichols R. H. and Hohenberg C. M. (1995) Origin and history of impact-melt rocks of enstatite chondrite parentage. *Geochim. Cosmochim. Acta* **59**, 161–175.

McCoy T. J., Dickinson T. L. and Lofgren G. E. (1999) Partial melting of the Indarch (EH4) meteorite: a textural, chemical, and phase relations view of melting and melt migration. *Meteorit. Planet. Sci.* **34**, 735–746.

McKinley S. G., Scott E. R. D. and Keil K. (1984) Composition and origin of enstatite in E chondrites. *Lunar Planet. Sci. Conf.* 14th, pp. B567–B572.

McSween H. Y. (1987) *Meteorites and Their Parent Planets*. Cambridge University Press, Cambridge, 237 pp.

Merrill G. P. (1915) On the monticellite-like mineral in meteorites, and on oldhamite as a meteoric constituent. *Proc. Natl. Acad. Sci. USA* **1**, 302–308.

Nickel E. H. and Nichols M. C. (1991) *Mineral Reference Manual*. Van Nostrand Reinhold, New York, 250 pp.

Olsen E. J., Huss G. I. and Jarosewich E. (1988) The Eagle, Nebraska, enstatite chondrite. *Meteoritics* **23**, 379–380.

Patzer A. and Schultz L. (2001) Noble gases in enstatite chondrites I: exposure ages, pairing, and weathering effects. *Meteorit. Planet. Sci.* **36**, 947–961.

Patzer A., Schlüter J., Schultz L., Tarkian M., Hill D. H. and Boynton W. V. (2004) New findings for the equilibrated enstatite chondrite Grein 002. *Meteorit. Planet. Sci.* **39**, 1555–1575.

Pryzlibski T. A., Zagożdżon P. P., Kryza R. and Pilski A. S. (2005) The Zaklodzie enstatite meteorite: mineralogy, petrology, origin and classification. *Meteorit. Planet. Sci.* **40**, A185–A200.

Rambaldi E. R., Rajan R. S. and Wang D. (1983) Chemical and textural study of Qingzhen, a highly unequilibrated enstatite chondrite (abstract). *Lunar Planet. Sci.* **14**, Lunar and Planetary Institute, Houston, pp. 626–627.

Rubin A. E. (1983a) Impact melt-rock clasts in the Hvittis enstatite chondrite breccia: implications for a genetic relationship between EL chondrites and aubrites. *Proc. Lunar Planet. Sci. Conf.* **14**, B293–B300.

Rubin A. E. (1983b) The Atlanta enstatite chondrite breccia. *Meteoritics* **18**, 113–121.

Rubin A. E. (1983c) The Adhi Kot breccia and implications for the origin of chondrules and silica-rich clasts in enstatite chondrites. *Earth Planet. Sci. Lett.* **64**, 201–212.

Rubin A. E. (1984) The Blithfield meteorite and the origin of sulfide-rich, metal-poor clasts and inclusions in brecciated enstatite chondrites. *Earth Planet. Sci. Lett.* **67**, 273–283.

Rubin A. E. (1997a) Sinoite (Si_2N_2O): crystallization from EL chondrite impact melts. *Am. Mineral.* **82**, 1001–1006.

Rubin A. E. (1997b) Igneous graphite in enstatite chondrites. *Mineral. Mag.* **61**, 699–703.

Rubin A. E. (2000) Petrologic, geochemical and experimental constraints on models of chondrule formation. *Earth Sci. Rev.* **50**, 3–27.

Rubin A. E. (2006) Shock and annealing in EL chondrites (abstract). *Meteorit. Planet. Sci.* **41**, A154.

Rubin A. E. and Keil K. (1983) Mineralogy and petrology of the Abee enstatite chondrite breccia and its dark inclusions. *Earth Planet. Sci. Lett.* **62**, 118–131.

Rubin A. E. and Scott E. R. D. (1997) Abee and related EH chondrite impact-melt breccias. *Geochim. Cosmochim. Acta* **61**, 425–435.

Rubin A. E., Scott E. R. D. and Keil K. (1997) Shock metamorphism of enstatite chondrites. *Geochim. Cosmochim. Acta* **61**, 847–858.

Rudneva A. V. and Panov A. S. (1962) The effect of calcium sulfide on the phase composition of slags in the system CaO–MgO–SiO_2. *Russ. Chem. Bull.* **11**, 510–513.

Scott E. R. D. (1982) Origin of rapidly solidified metal-troilite grains in chondrites and iron meteorites. *Geochim. Cosmochim. Acta* **46**, 813–823.

Sears D. W., Kallemeyn G. W. and Wasson J. T. (1983) Composition and origin of clasts and inclusions in the Abee enstatite chondrite breccia. *Earth Planet. Sci. Lett.* **62**, 180–192.

Sears D. W. G., Weeks K. S. and Rubin A. E. (1984) First known EL5 chondrite – evidence for a dual genetic sequence for enstatite chondrites. *Nature* **308**, 257–259.

Sneyd D. S., McSween H. Y., Sugiura N., Strangway D. W. and Nord G. L. (1988) Origin of petrofabrics and magnetic anisotropy in ordinary chondrites. *Meteoritics* **23**, 139–149.

Van Schmus W. R. and Wood J. A. (1967) A chemical-petrologic classification for the chondritic meteorites. *Geochim. Cosmochim. Acta* **31**, 747–765.

Wasson J. T. and Kallemeyn G. W. (1988) Compositions of chondrites. *Philos. Trans. R. Soc. Lond.* **A325**, 535–544.

Wheelock M. M., Keil K., Floss C., Taylor G. J. and Crozaz G. (1994) REE geochemistry of oldhamite-dominated clasts from the Norton County aubrite: igneous origin of oldhamite. *Geochim. Cosmochim. Acta* **58**, 449–458.

Zhang Y., Huang S., Benoit P. H. and Sears D. W. G. (1994) The unique thermal history of EL chondrites and a new means of classifying equilibrated enstatite chondrites (abstract). *Lunar Planet. Sci.* **25**, 1547–1548.

Zhang Y., Benoit P. H. and Sears D. W. G. (1995) The classification and complex thermal history of the enstatite chondrites. *J. Geophys. Res.* **100**, 9417–9438.

Zhang Y., Huang S., Schneider D., Benoit P. H., DeHart J. M., Lofgren G. E. and Sears D. W. G. (1996) Pyroxene structures, cathodoluminescence, and the thermal history of the enstatite chondrites. *Meteorit. Planet. Sci.* **31**, 87–96.

Associate editor: Gregory F. Herzog